Indian Geotechnical Journal, 18(4), 1988

Analysis of Cylindrical Storage Tank-Foundation Interaction Using Finite Element Method

by

M.M. Zaman*

I.U. Mahmood**

Introduction

THE analysis and design of circular foundations for cylindrical structures, such as storage tanks, tower silos, nuclear reactors, and chimneys, constitute a problem of practical importance in geotechnical engineering. In the conventional design/analysis methods, foundations are often treated as isolated units; thus, the interaction between the tank wall and the foundation, as well as between the foundation and the supporting soil medium, are essentially ignored or over-simplified. Although such assumptions may lead to considerable simplifications in the analysis and design, they may not be justified in many practical situations where the superstructure (tank wall) has significantly large stiffness and is rigidly connected to the foundation.

The main objective of this paper is to examine the response of a cylindrical storage tank-foundation system using the finite element technique, which considers the complete interaction between the tank wall, foundation and supporting soil medium (Fig. 1). Emphasis is given to accurately modeling the nonlinear deformation characteristics of the interface between the foundation and the soil medium using a special interface or joint element (Faruque 1980, Ghaboussi, *et al.*, 1973). Moreover, the non-linear behaviour of soil is taken into consideration by using the so-called hyperbolic constitutive relations (Desai and Siriwardane, 1984). Parametric studies are performed to assess the effects of some important factors, namely, depth of foundation embedment, interface roughness, soil nonhomogeneity and non-linearity, and relative rigidities of the tank wall-foundation and soil system. Numerical results are presented in a non-dimensional form which can be used readily for estimating responses of a wide variety of cylindrical tank foundations.

---

*Associate Professor, School of Civil Engineering and Environmental Science, University of Oklahoma, Norman, O.K. 73019, USA

**Graduate Research Assistant, School of Civil Engineering and Environmental Science, University of Oklahoma, Norman, OK 73019, USA.

(*The modified manuscript of this paper was received in September* 1988, *and is open for discussion till end of June*, 1989)

Review of Literature

The flexural behaviour of axisymmetrically loaded (isolated) circular plates has been analyzed by many investigators using various approaches (Finelli *et al.* 1984; Selvadurai, 1979*b*; Zaman *et al.*, 1988). Noteworthy developments in this area are due to Zemochkin (1939), Brown (1969), Hooper (1974, 1975), Selvadurai (1979*a*), and Issa (1985), among others. A comprehensive review on the subject is given by Selvadurai (1979*b*); only a brief review of some recent works that are directly relevant to the present paper is included here.

Although a substantial amount of studies have been done in the past on the analysis of (isolated) circular foundations, only a few studies have been done to address the complete interaction problem involving a cylindrical storage tank because of its complex nature. Booker and Small (1983) proposed an analytical technique based on the flexibility method to investigate the behaviour of cylindrical tanks resting on the surface of an isotropic elastic halfspace. The tank wall and the foundation were considered as a single unit. Also, this analysis is only applicable to cases where the radii of the tank wall and the foundation plate are equal. This assumption may not be justified in most practical situations.

More recently, Issa (1985), Issa and Zaman (1985) and Zaman, *et al.*, (1988) have investigated a similar problem using the energy approach in which the foundation plate and the tank wall may have different radii. However, it may be noted that both of these analyses focused on the response of surface foundations (*i.e.*, no embedment) only. The interface condition between the foundation and the halfspace was assumed to be perfectly smooth, and the soil medium was assumed to be isotropic, homogeneous, and elastic. In most practical situations, these assumptions are unrealistic.

In the present paper, a more realistic analysis procedure which circumvents some of the aforementioned limitations is presented. description of the proposed finite element procedure is given in the following and the numerical results are presented subsequently.

Proposed Analysis Procedure

For finite element idealization, the cylindrical storage tank-foundation-soil system in Fig. 1 is treated as an axisymmetric problem. Other assumptions involved in the formulation are listed below:

1. Thin plate and thin shell theories (Timoshenko, *et al.*, (1959)) are used to describe the flexural behavior of the foundation plate and the tank wall, respectively. Displacements are assumed to be small and the material behaviour is to be linearly elastic.

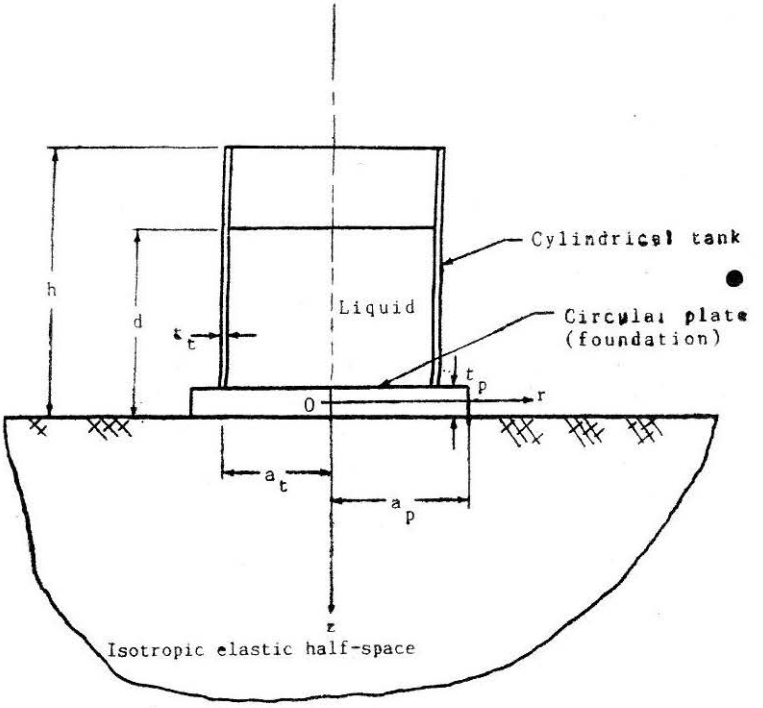

FIGURE 1 Schematic Representation of the Cylindrical Liquid Storage Tank-Plate-Soil System

2. The junction between the tank wall and foundation is rigid; relative displacement and/or rotation is not permitted at the junction.
3. The nonlinear behaviour exhibited by the interface (see Fig. 1) is idealized by using elastic perfectly plastic constitutive relations (Fig. 2).
4. The peak shear strength is a function of interface normal stress, cohesion, and roughness as measured by the interface friction angle.
5. Interfaces cannot sustain any tensile (normal) stress (Fig. 2).
6. Interfaces are nondilatant and do not show any strain softening behaviour.
7. The thickness of the interface element is small compared to its length.

Modeling of Tank Wall and Foundation Plate

The cylindrical tank wall is modelled using axisymmetric thin shell element (Bathe 1982, Zienkiewicz 1971), and annular plate elements are

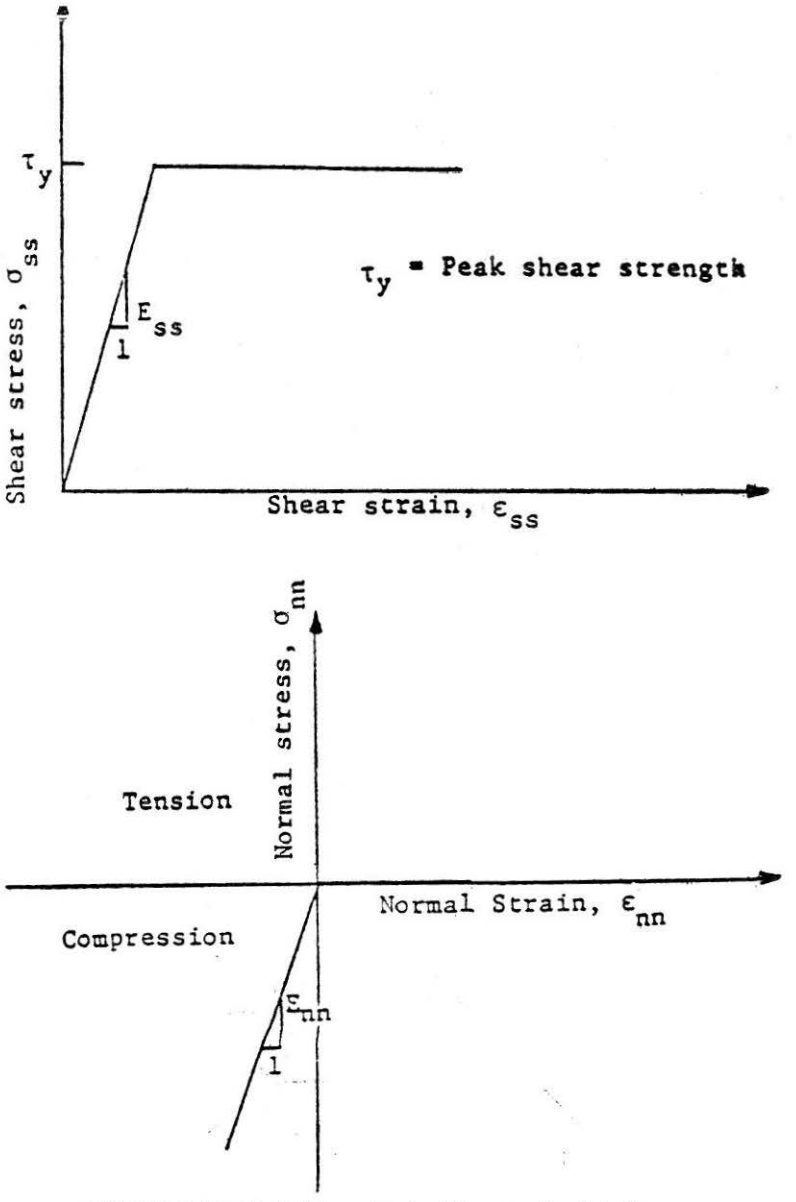

FIGURE 2 Idealized Stress-Strain Diagram for Interface.

used to model the flexural behavior of the foundation plate. A special formulation is adopted for the central foundation region (Faruque 1980). As the stiffness matrices for such elements can be derived easily following the standard steps of finite elements (Bathe 1982, Zienkiewicz 1971), details are not given here.

Modeling of Frictional Behaviour of Interfaces

A four noded axisymmetic interface element developed originally by Ghaboussi *et al.*, (1973) and modified subsequently by Selvadurai and Faruque (1981) is further modified in the present study and employed to model the frictional behavior of soil-foundation interfaces. A schematic diagram of the element is shown in Fig. 3. As the thickness of the interface element is taken to be very small compared with its length, the strains across the element can be assumed as constant. Along the length of the element, a linear variation of strain is assumed.

Referring to Fig. 3, the interpolation functions for the interface element are assumed as

$$h_1 = (1 - \xi)/2 \; ; \; h_2 = (1 + \xi)/2 \qquad \ldots(1)$$

in which ξ is the local coordinate as shown.

Using the notations of Fig. 3 and following the standard steps of displacement finite element approach (Bathe (1982), Mahmood (1984)),

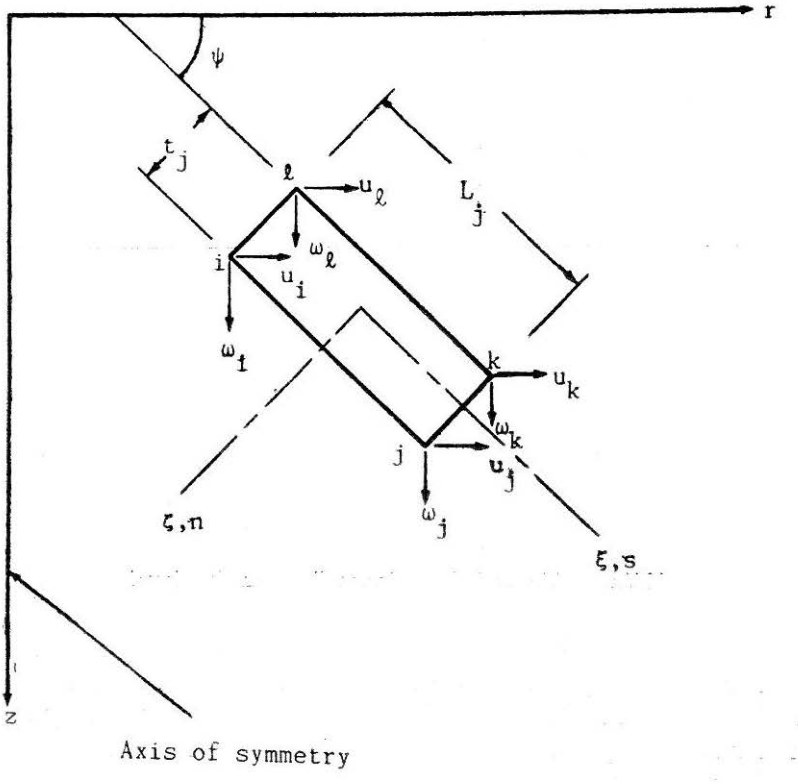

FIGURE 3 Four Noded Axisymmetric Interface Element Used.

the element stiffness matrix, $[K_i]$, for the interface element can be expressed in the form:

$$[K_i] = \int_v [B_i]^T [D_i] [B_i] \, dV \qquad \ldots(2)$$

where $[B_i]$ = strain — (relative) displacement transformation matrix given by (Ghaboussi, *et al.*, 1973; Mahmood (1984)) :

$$[B_i] = \begin{bmatrix} -B_1 & -B_2 & -B_3 & -B_4 & B_3 & B_4 & B_1 & B_2 \\ B_2 & -B_1 & B_4 & -B_3 & -B_4 & B_3 & -B_2 & B_1 \\ B_5 & 0 & B_6 & 0 & B_6 & 0 & B_5 & 0 \end{bmatrix} \qquad \ldots(3)$$

and

$$B_1 = \frac{h_1 \cos \psi}{t_i} \qquad \ldots(4a)$$

$$B_2 = \frac{h_1 \sin \psi}{t_i} \qquad \ldots(4b)$$

$$B_3 = \frac{h_2 \cos \psi}{t_i} \qquad \ldots(4c)$$

$$B_4 = \frac{h_2 \sin \psi}{t_i} \qquad \ldots(4d)$$

$$B_5 = \frac{h_1}{2r} \qquad \ldots(4e)$$

$$B_6 = \frac{h_2}{2r} \qquad \ldots(4f)$$

Also, in Eq. (2) the superscript T represents transpose and $[D_i]$ = constitutive relation matrix for the interface given by

$$[D_i] = \begin{bmatrix} E_{ss} & 0 & 0 \\ 0 & E_{nn} & 0 \\ 0 & 0 & E_{\theta\theta} \end{bmatrix} \qquad \ldots(5)$$

where E_{ss} and E_{nn} are, respectively, the interface shear and normal modulii. As suggested by Ghaboussi *et al.*, (1973), $E_{\theta\theta}$ is assumed as zero because of the uncertainty in estimating a realistic value for it.

Simulation of Deformation Modes

In the present study an interative technique is employed to simulate various modes of deformation such as stick, sliding, separation and rebonding that an interface element may undergo. A brief description of the algorithm used for the simulation of these modes is given in the following:

For an element in stick or no-slip mode—

$$\sigma_{nn} > 0, \text{ and}$$
$$|\sigma_{ss}| < \tau_y \qquad \ldots(6)$$

where σ_{nn} = average normal stress (compression is considered positive), σ_{ss} = average shear stress and τ_y = peak shear strength (of interface) as shown in Fig. 2. τ_y is considered positive here.

In order to initiate slip or sliding, the normal stress would still be compressive and the shear stress would be equal to the peak shear strength. Thus, for an element in the slip mode:

$$\sigma_{nn} > 0, \text{ and}$$
$$|\tau_{ss}| \geqslant \tau_y \qquad \ldots(7)$$

It may be noted that the condition $|\sigma_{ss}| > \tau_y$ is not practically possible because τ_y is the peak shear strength of the element. If during an analysis σ_{ss} becomes larger than the peak strength, τ_y, then the resulting deformation is considered to be kinematically inadmissible. An iterative scheme is adopted so that after the convergence of iteration, the stress components satisfy the following conditions:

$$\sigma_{nn} > 0, \text{ and}$$
$$|\sigma_{ss} \cong \tau_y \qquad \ldots(8)$$

In the case of debonding or separation mode, the stress conditions will be of the form:

$$\sigma_{nn} \cong 0, \text{ and}$$
$$|\sigma_{ss}| \cong 0 \qquad \ldots(9)$$

As in the case of the sliding mode, here also one may find that the computed normal and shear stresses have violated the conditions of Eq. (9). Once again for such a situation, iteration must be performed so as to make the deformation of the interface acceptable. After convergence is achieved, the resulting deformation should approximately satisfy Eq. (9).

As indicated by Eq. (10), the rebonding mode is assumed to have taken place when the interface shearing stress becomes non-zero and the normal stress, which was tensile previously, becomes compressive in the subsequent loading.

$$\sigma_{nn} > 0$$
$$|\sigma_{ss}| \geqslant 0 \text{ and } |\sigma_{ss}| \leqslant \tau_y \qquad \ldots(10)$$

The following steps illustrate the scheme used in this study for incorporation of various modes of deformation.

1. An interaction problem is first discretized into finite elements. The stiffness matrices for structure (foundation plate and tank wall in this case), soil, and interface elements are formed and assembled to obtain the global stiffness matrix $[K]$. The global consistent load vector $\{F\}$ is formed and the system of the linear equation $[K]\{u\} = \{F\}$ is solved to obtain the nodal displacements, $\{u\}$.

2. The average normal stress (σ_{nn}) of an element is calculated by the following expression (see Fig. 3):

$$\sigma_{nn} = -\frac{E_{nn}}{2t_i}[(u_l - u_i + u_k - u_j)\sin\psi + (\omega_i - \omega_l + \omega_j - \omega_k)\cos\psi] \quad \ldots(11)$$

where E_{nn} = normal stiffness, t_i = thickness of the element and u_i, ω_i etc. are the nodal displacements of node i in the radial and the vertical directions, respectively.

Average shear stress (σ_{ss}) of the joint element is calculated from the following expression (Fig. 3):

$$\sigma_{ss} = -\frac{E_{ss}}{2t_i}[(u_l - u_i + u_k - u_j)\cos\psi + (\omega_i - \omega_l + \omega_j - \omega_k)\sin\psi] \quad \ldots(12)$$

where E_{ss} = shear stiffness of the element.

3. If σ_{nn} calculated in step 2 is tensile, then the peak shear strength of the interface (τ_y) is set equal to zero, otherwise, τ_y is calculated from the Mohr—Coulomb criterion (Desai and Siriwardane (1984)):

$$\tau_y = c + \sigma_{nn}\tan\phi \quad \ldots(13)$$

where c = cohesion of the interface element, σ_{nn} = normal stress calculated in step 2, and ϕ = angle of internal friction for the interface element. In the numerical results presented here, the following values were used to represent the smooth and the bonded interfaces: $c = 0$, $\tan\phi = 0.001$ for smooth case, and $c = 0$, $\tan\phi = 10.0$ for bonded case.

4. The status of each interface element is checked by using the appropriate aforementioned equations. If the normal stress σ_{nn} becomes tensile the resulting vector (F) is calculated as follows.

$$F_n = \pi(r_j + r_i)L_j\sigma_{nn} \quad \ldots(14)$$

where L_j = length of the joint element, and r_i and r_j are the radial coordinates of nodes i and j, respectively.

This excess force F_n can be converted to self-equilibrating nodal forces. The term "self-equilibrating" is used to indicate that these forces balance each other internally and may be expressed as

$$F_{in} = \frac{-\pi L_j}{2}\left(\frac{3r_i + r_j}{2}\right)\sigma_{nn}$$

$$F_{jn} = \frac{-\pi L_j}{2}\left(\frac{r_i + 3r_j}{2}\right)\sigma_{nn} \qquad \ldots(15)$$

$$F_{kn} = -F_{jn}$$

$$F_{ln} = -F_{in}$$

$$F_{is} = F_{js} = F_{ks} = F_{ls} = 0$$

These forces are then transformed to the global coordinate system by using an appropriate transformation (Mahmood (1984)).

Likewise, for the excess shear stress $|\sigma_{ss} - \tau_y|$, the excess shear force (V_s) is calculated by

$$V_s = \pi L_j (r_j + r_i)(|\sigma_{ss}| - \tau_y) \qquad \ldots(16)$$

and is converted to nodal forces in the global system in a similar manner.

5. Using the aforementioned self-equilibrating nodal forces, wherever appropriate, the global force vector $\{F\}$ is modified. Let the modified force vector be represented by $\{F_m\}$. With this force vector $\{F_m\}$, the equilibrium equation $[K]\{u_m\} = \{F_m\}$ is solved again to obtain the modified displacement vector $\{u_m\}$. The steps 2 through 4 are repeated in this manner until convergence is reached.

It should be noted that in the analysis bonded or smooth condition is simulated by assigning a relatively high or a low value of peak shear strength, respectively. Since peak shear strength is a function of c and ϕ, these values were chosen to generate either very high or very low peak shear strength. For an analysis, the suitability of c and ϕ was justified by checking the stress condition in the interface elements.

Idealization of Soil Medium

The soil medium is considered as an isotropic and nonlinear elastic material, and is discretized by using axisymmetric solid elements of (three noded) triangular cross section. The nonlinear stress-strain behaviour of

soil is represented by the widely used hyperbolic model proposed by Kondner and his co-worker (1963*a*, 1963*b*):

$$\sigma_1 - \sigma_3 = \frac{\varepsilon}{a + b\varepsilon} \qquad \ldots(17)$$

where σ_1 and σ_3 are the major and the minor principal stresses, respectively, ε is the strain in the direction of major principal axis, and a and b are associated material parameters.

Because stress is expressed as a nonlinear function of strain, in the hyperbolic model, an iterative approach must be used to incorporate this model in an analysis procedure. Figure 4 shows the schematic of the iteration algorithm used in this study. It may be noted that the secant modulus is used here instead of the tangent modulus. The secant modulus seems more appropriate because it provides faster convergence. Also, it is feasible because the response only due to total loading is desirable. It should be noted that secant modulus approach may not be appropriate if insitu stresses are considered in the analysis. In the present analysis insitu stresses were not incuded. The major steps involved in the interation scheme are outlined in the following steps (Mahmood 1984, Zaman, *et al.*, 1985):

1. For a given problem, the stiffness matrices for the shell, plate, interface and soil are evaluated and assembled to form the global

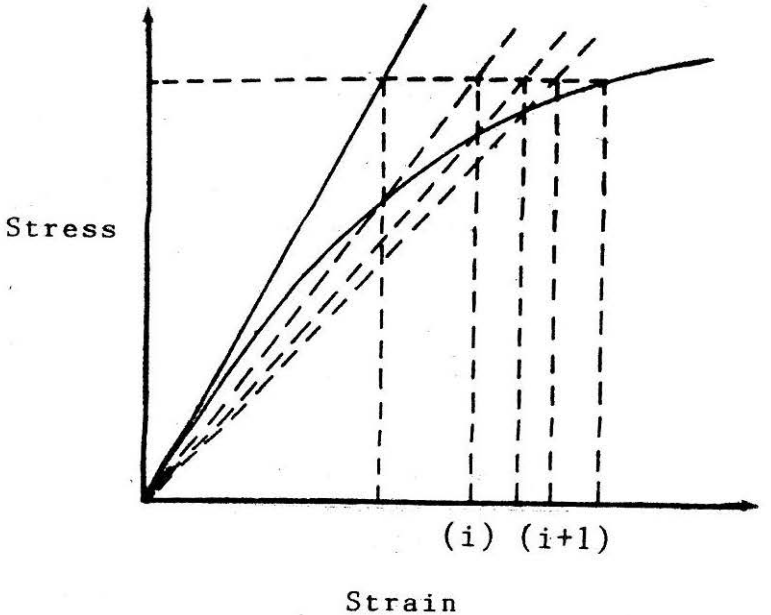

FIGURE 4 Technique for Approximating Nonlinear Behavior by Successive Iterations

stiffness matrix $[K]$. The stiffness matrices for the soil elements are derived on the basis of the initial tangent modulus $(E_t)_i$ (Fig. 4) and the Poisson's ratio v_s. The force vector $\{F\}$ for the total system is derived by using consistent load vectors (Zienkiewicz (1971)). The system of linear simultaneous equations $[K]\{u\} = \{F\}$ is then solved to determine the global nodal displacement vector $\{u\}$.

2. The nonlinear solution technique, described previously, which accounts for interface nonlinearity is employed to modify the displacement vector $\{u\}$.

3. Utilizing the displacement vector $\{u\}$ obtained in step 2, strain and stress components for each element are calculated. Let $(\sigma_{rr})^i$, $(\sigma_{zz})^i$, $(\tau_{rz})^i$, $(\sigma_{\theta\theta})^i$, $(\varepsilon_{rr})^i$, $(\varepsilon_{zz})^i$, $(\gamma_{rz})^i$, and $(\varepsilon_{\theta\theta})^i$, be the stress and strain components be for a given element, i.

   Based on these components, the principal stress and strain components are calculated. Let the major and minor normal principal stress components be denoted by σ_1^i and σ_3^i, respectively and the corresponding major principal strain be denoted by ε_p^i. Likewise, the major stress difference is indicated by $(\sigma_1^i - \sigma_3^i)_c$, where the subscript c stands for computed stress.

4. Using the hyperbolic relationship of Eq. (17), $(\sigma_1^i - \sigma_3^i)_m$ is calculated. The subscript m represents the model predicted stresses. If

$$\left[\frac{\{(\sigma_1^i - \sigma_3^i)_c - (\sigma_1^i - \sigma_3^i)_m\}^2}{(\sigma_1^i - \sigma_3^i)_c^2}\right]^{\frac{1}{2}} > \bar{\varepsilon}_t \qquad \ldots(18)$$

where $\bar{\varepsilon}_t$ is a preassigned small number, called the tolerance, then a modified estimate of the secant modulus is made.

$$E_m^i = \frac{(\sigma_1^i - \sigma_3^i)_m}{\varepsilon_p^i} \qquad \ldots(19)$$

If

$$\left[\frac{\{(\sigma_1^i - \sigma_3^i)_c - (\sigma_1^i - \sigma_3^i)_m\}^2}{(\sigma_1^i - \sigma_3^i)_c^2}\right]^{\frac{1}{2}} < \bar{\varepsilon}_t \qquad \ldots(20)$$

no modification is done for this element, and the check is continued for the next element.

It may be noted that the assumed value for the tolerance ($\bar{\varepsilon}_t$) will depend on the magnitude of the principal stresses $(\sigma_1^i - \sigma_3^i)_c$. From several trial runs a value of $(\bar{\varepsilon}_t)/(\sigma_1^i - \sigma_3^i)_c^2 = 0.05$ was found to be adequate.

5. With the modified secant modulii, stiffness matrices for the soil elements are formed and added to the stiffness matrices of the foundation plate, shell and interface elements to form the revised global stiffness matrix, and steps 1 through 4 are repeated.

6. When none of the soil elements need modifications, the convergence is assumed to have been achieved, and the iteration is terminated.

7. Another criterion used for terminating the interative scheme is that when the number of iteration equals a preassigned number.

8. With the displacements obtained in the final iteration, stresses in the foundation plate, shell (tank wall), and soil are calculated and printed out.

Numerical Results

The finite element formulation described in the preceding section has been incorporated in a computer code, written in FORTRAN language for solving soil-structure interaction problems with plane stress, plane strain; or axisymmetric idealization. The computer code has been extensively used for solving a number of soil-structure interaction problems, and accuracy of numerical results has been verified wherever possible (Mahmood, 1984; Zaman, *et al.*, 1985). Some pertinent numerical results for the liquid storage tank-foundation-soil interaction problem (Fig.1) under consideration are presented in this section. Additional results are given by Mahmood (1984).

Comparison of Results

The liquid storage tank problem analyzed by Booker and Small (1983) and Issa (1985) is solved here using the aforementioned code for the purpose of comparison. The interface condition is assumed to be smooth. Figure 5 shows a comparison for plate deflection. Although the basic nature of the deflected shape obtained from both methods is similar, some difference in magnitude is observed, especially in the central region of the foundation plate. This difference is probably caused by the boundary conditions used in the formation of both methods. In the finite element method, no restriction on the bending moment at the wall foundation junction can be imposed directly, while in the energy method (Issa (1985), Issa and Zaman (1985)) such restrictions are imposed. Although no results are presented here, the contact pressure variation compared well with that of Booker and Small (1983).

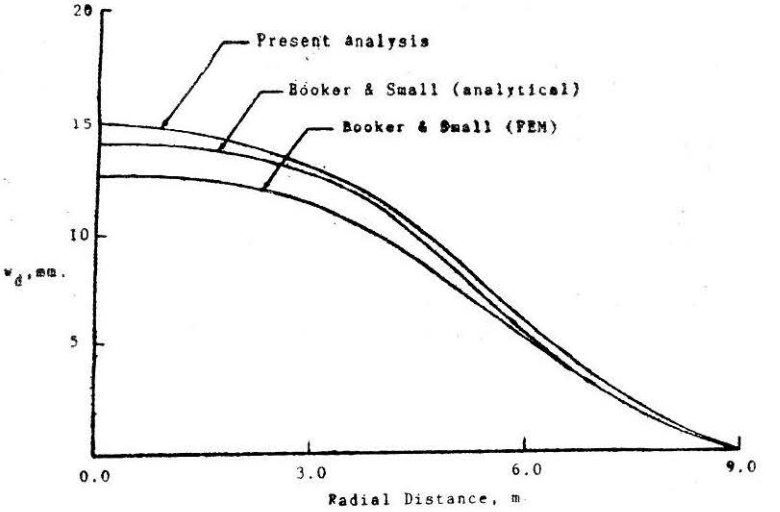

FIGURE 5 Variation of Differential Plate Displacements and comparisons with Booker and Small (1983) and Issa (1985).

Similar comparison for plate radial moment distribution is shown in Fig. 6. Overall, the values compare favourably except near the tank wall-foundation junction. It is believed that this difference is caused due to different boundary conditions at the wall-foundation junction. Because no exact solution is available for this problem, only qualitative comparison is plausible.

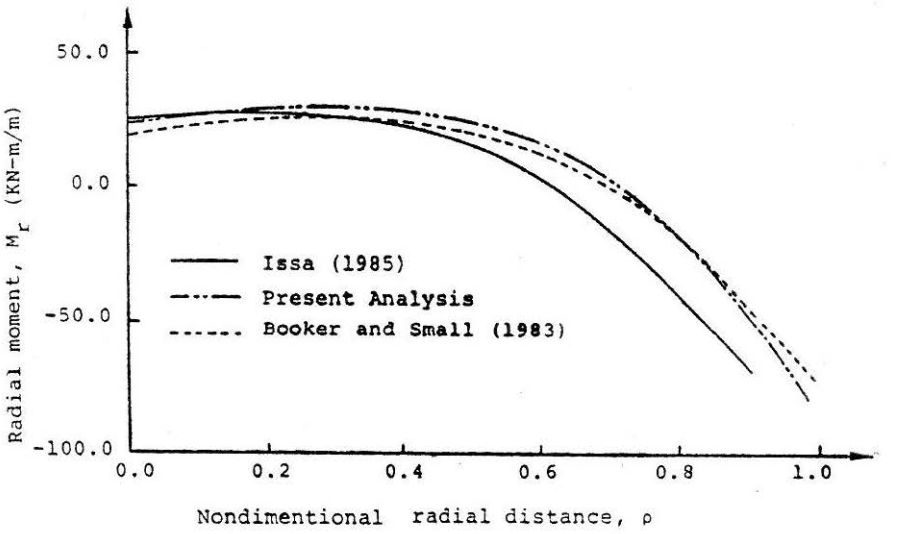

FIGURE 6 Variation of Radial Moments and Comparison of Results with Booker and Small (1983) and Issa (1985).

The accuracy of finite element results obtained from the present study also compared with similar results reported by Brown (1969), for isolated foundations (without tank-walls). For $k_p = 1$ (see Eq. 21), the present analysis yields a value of 0.20 for the maximum differential deflection (non-dimensional), compared to 0.18 reported by Brown (1969). For $k_p = 10$, which represents a more rigid foundation, the corresponding values are 0.03 and 0.029, respectively. For a relatively flexible foundation ($k_p = 0.1$), the differential deflection predicted by the present analysis (0.47) was less than that reported by Brown (0.55); however, a flexible foundation of such low relative rigidity (k_p) does not seem to have any practical application.

Parametric Study

The behavior of circular foundations can be significantly influenced by the relative rigidity of the tank-wall-foundation system. For a tank wall of high (flexural) stiffness, the rotation at the wall-foundation junction may be considered negligible, while for a flexible wall-foundation system, the junction may experience finite rotation. Similarly, it is conceivable that the amount of interaction will depend upon the relative rigidity of the foundation plate-soil system. Thus, for convenience in parametric study, the following relative rigidity factors are defined (Issa 1985, Issa and Zaman 1985):

$$K_p = (1 - \nu_s^2)\left(\frac{E_p}{E_s}\right)\left(\frac{t_p}{a_p}\right)^3 \qquad \ldots(21)$$

$$K_t = (1 - \nu_s^2\left(\frac{E_t}{E_s}\right)\left(\frac{t_t}{a_t}\right)^3 \qquad \ldots(22)$$

where K_p = relative rigidity of plate-soil system, K_t = relative rigidity of wall-soil system, a_t = radius of tank, a_p = radius of plate, t_t = tank wall thickness, t_p = plate thickness, and E and ν represent the elastic modulus and Poisson's ratio, respectively. The subscripts t, p, and s stand for tank wall, foundation plate, and soil medium, respectively. In the parametric study, K_p and K_t were chosen to cover plates and walls of very flexible to very rigid type. The Poisson's ratios for the tank wall and the foundation plate were kept constant. Previous studies (Issa 1985) have shown that the Poisson's ratio of the superstructure does not have significant influence on the foundation response.

For convenience, numerical results are presented in a non-dimensional form:

$$w_o = \frac{p\, a_p}{E_s}\, \bar{w} \qquad \ldots(23a)$$

$$w_d = \frac{p\, a_p}{E_s}\, \bar{w}_d \qquad \ldots(23b)$$

$$M_o = p\, a_p^2\, \bar{M}_o \qquad \ldots(23c)$$

where p = uniformly distributed load on the plate, w_o = central plate deflection, w_d = differential plate deflection and M_o = radial moment at plate centre, and an over-bar represents non-dimensional quantities.

Elastic and Homogeneous Soil Medium

Figure 7 shows the variation of central deflection $\bar{w}_o$ with K_t. It is observed that the central deflection of the plate decreases with increasing K_t. When K_t is changed from .001 to 0.1, $\bar{w}_o$ decreased by about 2.5% when the Poisson's ratio of soil (ν_s) equaled 0 for a bonded (plate-soil) interface condition. For $\nu_s = 0.4$, this difference is about 3%. As may be expected, at a particular ν_s and K_t, the deflection is higher for smooth plate-soil contact; for $\nu_s = 0.0$ and $K_t = 0.1$, the difference for the different contact conditions is 5.55%. For the same relative rigidity but with $\nu_s = 0.4$, the difference is only 0.43%. The effect of the interface condition become insignificant as the elastic half-space becomes more incompressible (*i.e.*, ν_s approaches 0.5). Figure 8 shows the variation of the maximum differential plate displacement with the relative rigidity of plate. As in the case of total (foundation) deflection, the differential deflection ($\bar{w}_d$) also is affected more due to a change in the interface condition at a lower ν_s. As may be expected, at $K_t = 0.1$, $\bar{w}_d$ for the smooth case is 6.26% higher for $\nu_s = 0.0$, where as for $\nu_s = .4$, the difference is negligible. Central plate moment ($\bar{M}_o$) variation with K_t is plotted in Fig. 9. $\bar{M}_o$ increases with increasing K_t. The interface condition is prominent at a lower ν_s.

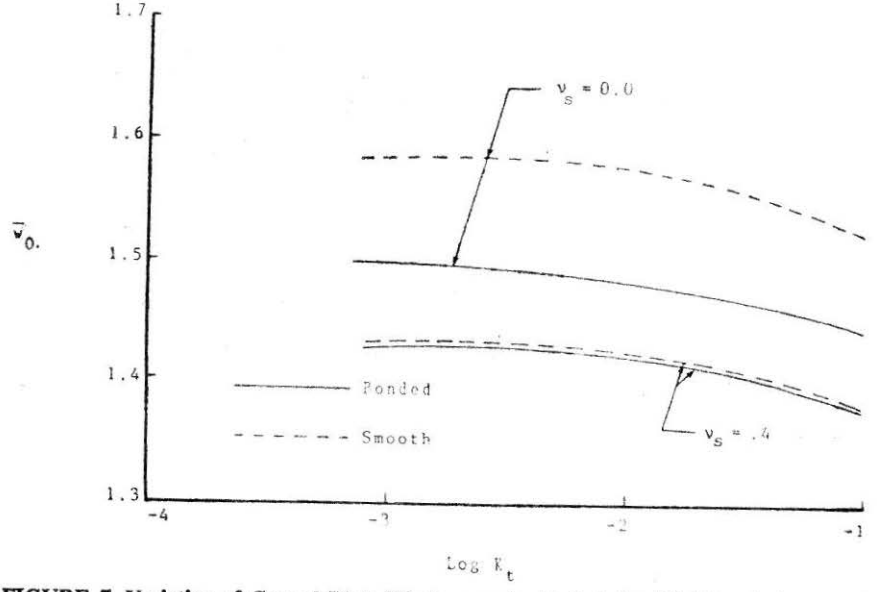

FIGURE 7 Variation of Central Plate Displacement with Relative Rigidity of Tank Wall.

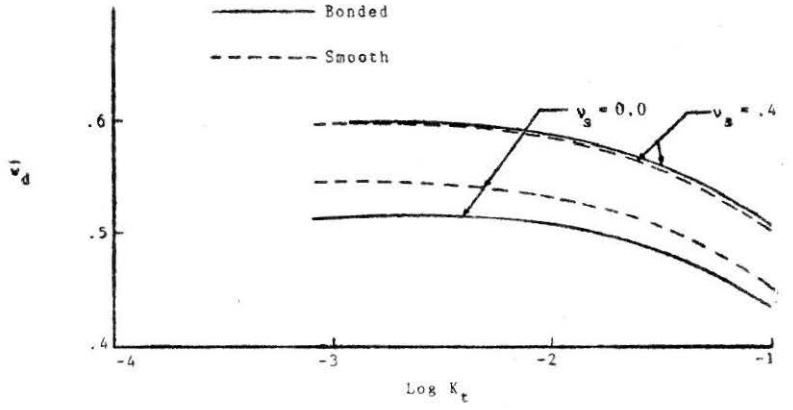

FIGURE 8 Variation of Maximum Differential Plate Displacement with Relative Rigidity of Tank Wall.

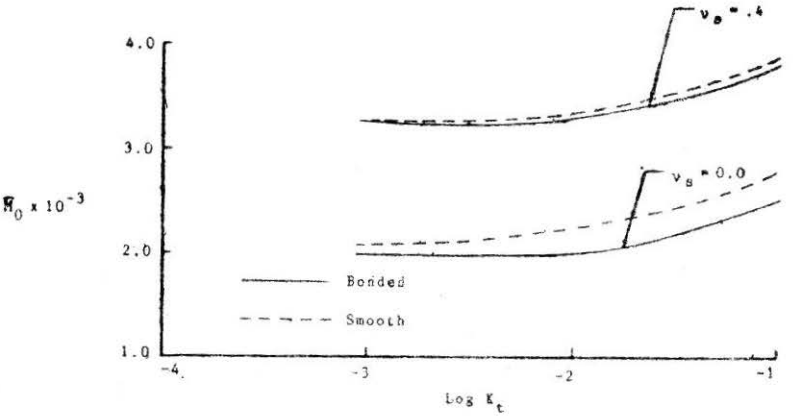

FIGURE 9 Variation of Central Plate Moment with Relative Rigidity of Tank Wall.

As mentioned before, the response of a cylindrical tank foundation can be significantly affected by the relative rigidity of the plate-soil (K_p) system. To investigate this effect the problem at hand is solved for different K_p, and the results are shown in Figs. 10 through 12. Figure 10 shows the variation of $\bar{w}_o$ with K_p. For $\nu_s = 0.0$ and bonded interface, $\bar{w}_o$ decreases as much as 26.4% by increasing K_p from .01 to 10. At any particular K_p, $\bar{w}_o$ is larger for smooth plate-soil contact, and this difference is larger at a lower ν_s. For $\nu_s = 0$ at $K_p = .05$, the difference is 5.42% while it is only 0.43% at $\nu_s = 0.4$. Figures 11 and 12 show the variation of maximum differential plate deflection and central moment, respectively, with K_p. $\bar{w}_d$ decreases as the plate becomes rigid and approaches a zero value at $K_p = 10$. $\overline{M_o}$ increases significantly with increasing K_p, and by changing K_p from 1 to 10, an almost 120% increase in $\overline{M_o}$ is observed at $\nu_s = 0.4$. The effect of the contact condition is more significant at a lower ν_s.

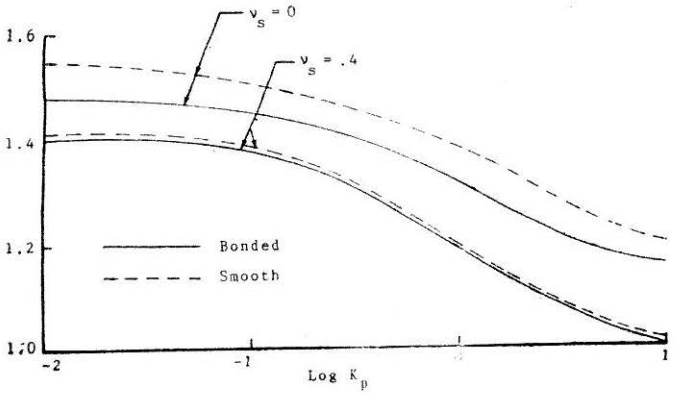

FIGURE 10 Variation of Central Plate Displacement with Relative Rigidity of Plate.

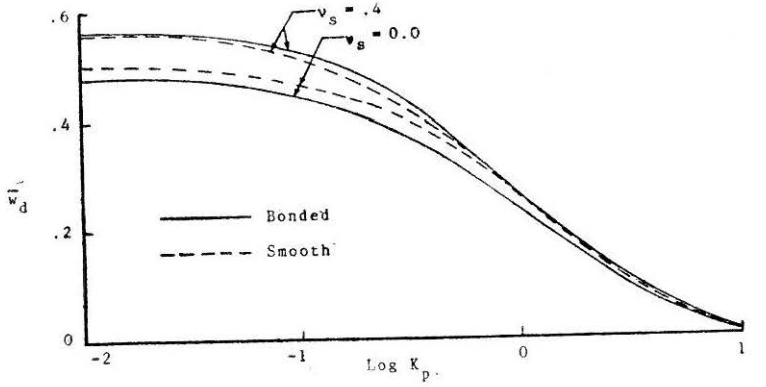

FIGURE 11 Variation of Maximum Differential Plate Displacement with Relative Rigidity of Plate.

Partially Embedded Foundation: The results discussed so far were obtained from the analysis of a liquid storage tank resting on the surface of an isotropic homogeneous elastic halfspace. In an actual situation, a structural foundation seldom rests on the surface of the elastic halfspace. Most foundations are embedded in the halfspace, and their interaction may be significantly different from the case where the plate is resting on the surface. Realizing the importance of depth of embedment, the response of a partially embedded liquid storage tank shown in Fig. 13 is investigated, and the significant features are discussed below. It may be noted that for the partially embedded case, interface elements were used both at the bottom and the sides of the storage tank.

Figure 14 shows the variation of $\bar{w}_o$ with K_t. The response of a surface plate is also plotted in the same figure for comparison. It is seen that effect of interface is more significant for the embedded plate. At $K_t = .001$

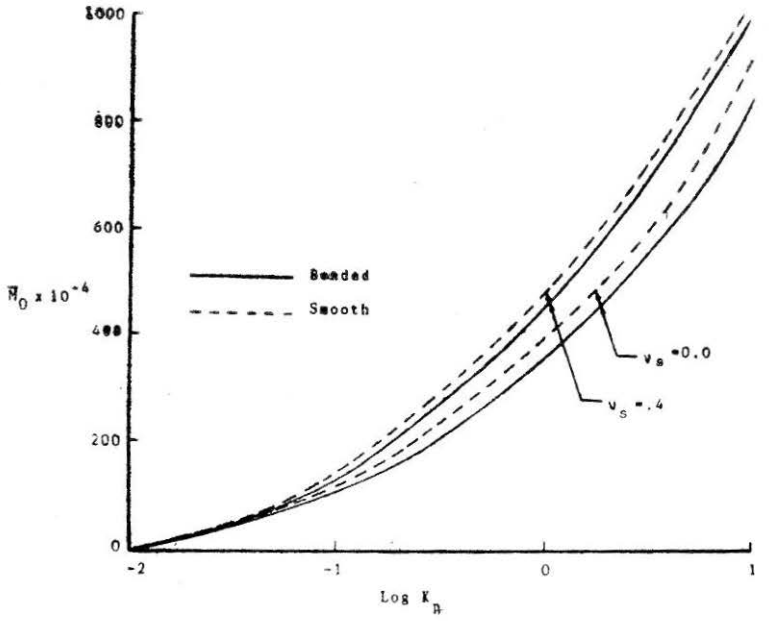

FIGURE 12 Variation of Central Plate Moment with Relative Rigidity of Plate.

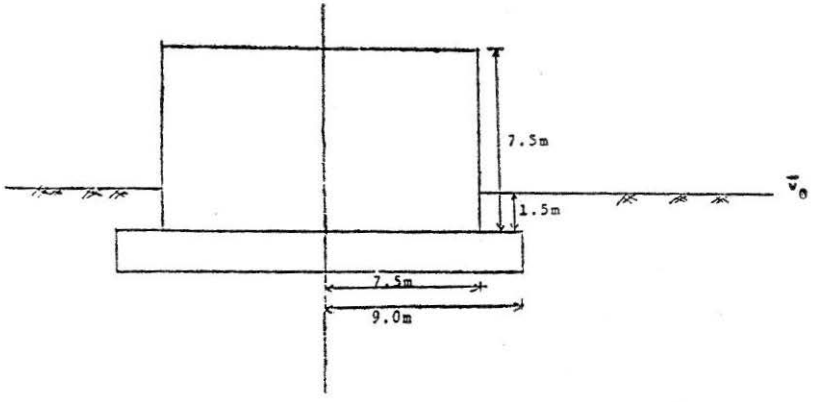

FIGURE 13 Partially Embedded Storage Tank Resting on Isotropic Half-Space.

and $\nu_s = 0.30$, $\bar{w}_o$ is 0.81% higher for smooth contact as compared to bonded contact in case of the surface plate whereas it is about 5.8% higher for an embedded plate. A similar trend is observed for maximum differential displacement (Fig. 15) and central moment (Fig. 16). For identical conditions, $\bar{w}_o$ is appreciably lower and the central moment is higher for an embedded plate. Similar comparisons between surface and embedded plates for varying K_p is shown in Figs. 17 through 19. In this study, prominance of wall-plate-soil interaction in the case of an embedded plate is established.

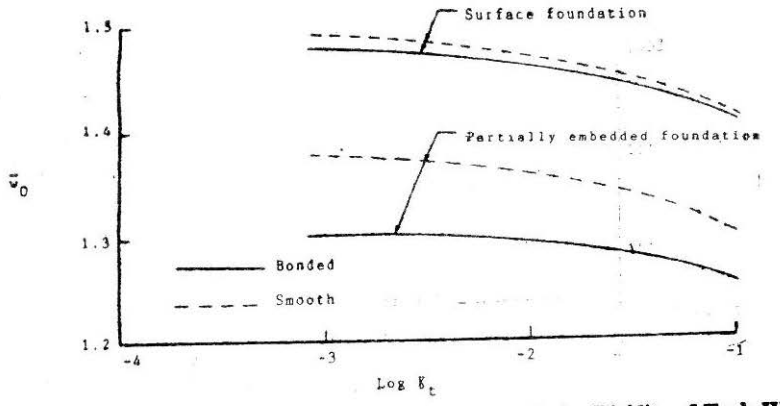

FIGURE 14 Variation of Central Plate Displacement with Relative Rigidity of Tank Wall, for $V_s = .3$.

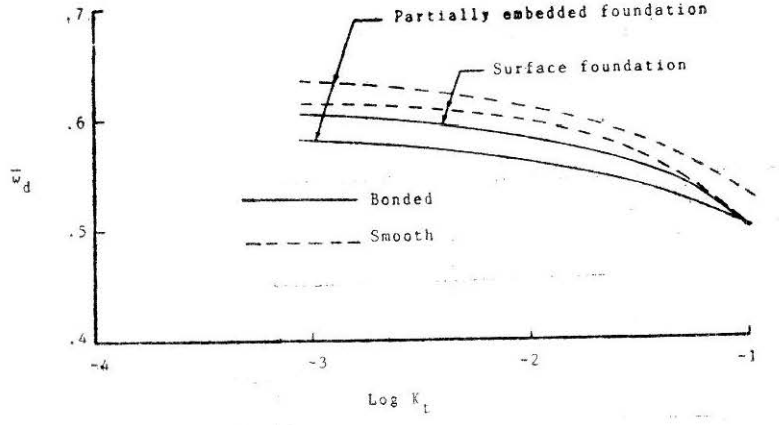

FIGURE 15 Variation of Maximum Differential Plate Displacement with Relative Rigidity of Tank Wall, for $V_s = .3$.

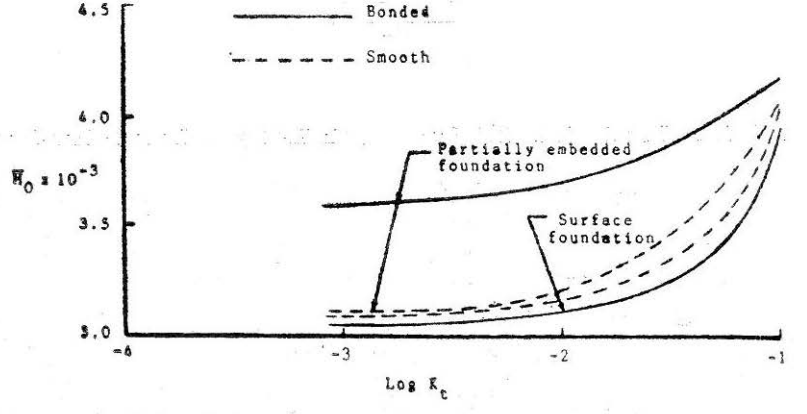

FIGURE 16 Variation of Central Plate Moment with Relative Rigidity of Tank Wall, for $V_s = .3$.

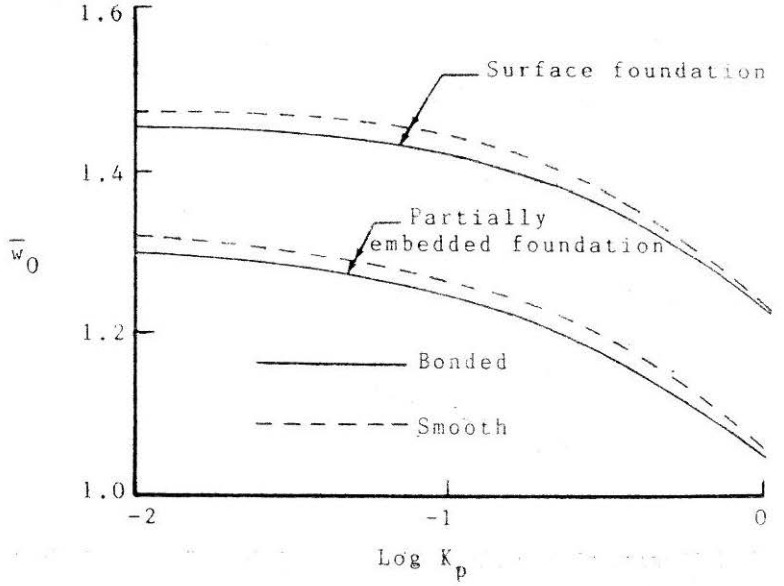

FIGURE 17 Variation of Central Plate Displacement with Relative Rigidity of Plate, for $V_s = .3$.

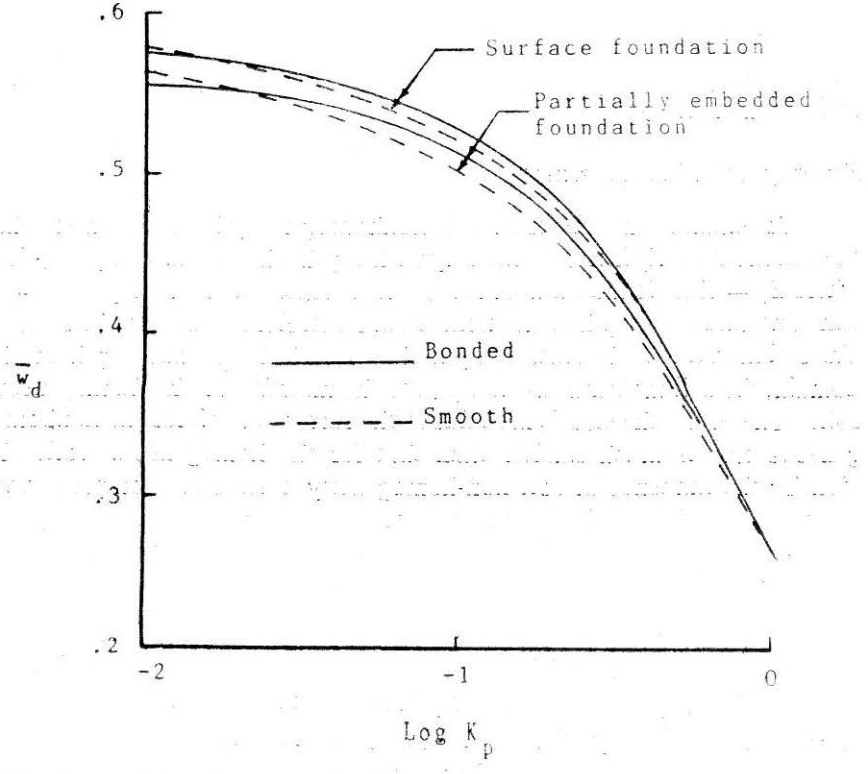

FIGURE 18 Variation of Maximum Differential Plate Displacement with Relative Rigidity of Plate, for $V_s = .3$.

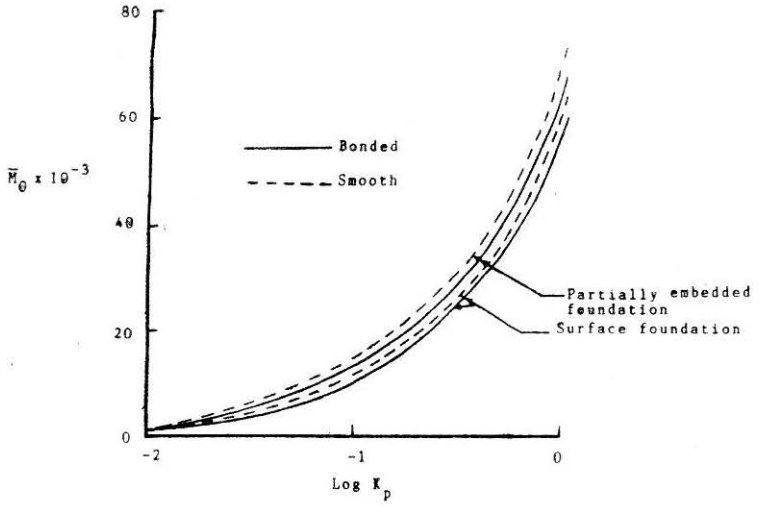

FIGURE 19 Variation of Central Plate Moment with Relative Rigidity of Plate for V_s=0.30.

The results of parametric studies presented in this section lead to certain specific conclusions. In general, the relative rigidity parameter K_t has less influence on plate response compared to the relative rigidity para-parameter K_p. The interaction is more prominent at a lower Poissons' ratio of the halfspace.

Effect of Soil Nonhomogeneity

To examine the effects of soil nonhomogeneity it is assumed that the soil modulus E_h increases linearly with depth; that is $E_h = E_s(1 + \lambda h)$, where E_s = Elastic modulus of soil at the surface of the halfspace, $\lambda = a$ constant, and h = depth of the centroid of a soil element below the surface. The soil modulus at the surface, E_s, is chosen such that at mid-depth of the domain, the soil modulus, E_h, is equal to the modulus of the homogeneous soil. Therefore, the elastic modulus at the surface of soil for the nonhomogeneous case is much smaller than that for the homogeneous soil. To identify the influence of soil non-homogeneity, results are compared with the corresponding results for the case of homogeneous soil. Some typical results are presented in Figs. 20 through 22. The following numerical values were used in this study: $E_s = 10\ MPa$ and $\lambda = .1$ per meter.

It is observed that the responses obtained for the non-homogeneous soil assumption are much higher than the corresponding responses obtained from the homogeneous soil assumption, the difference being reduced at higher relative rigidity of the tank wall. The effect of the interface is seen to be more prominent in case of the nonhomogeneous soil assumption. The responses for different plate relative rigidities also show a similar pattern

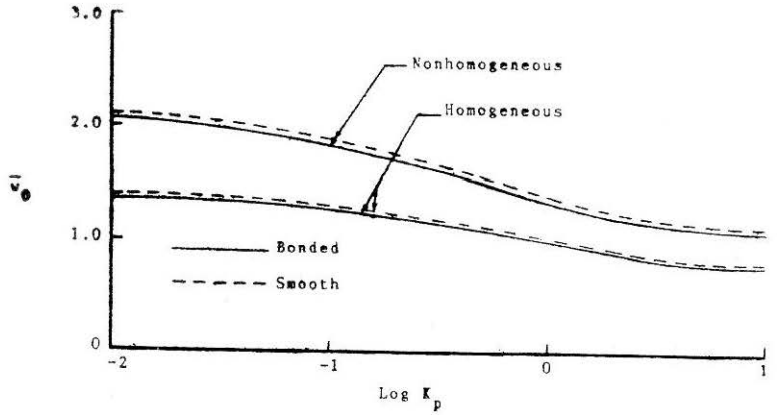

FIGURE 20 Effect of Nonhomogeneity and K on the Variation of Central Displacement of a Partially Embedded Foundation, for $V_s=0.3$.

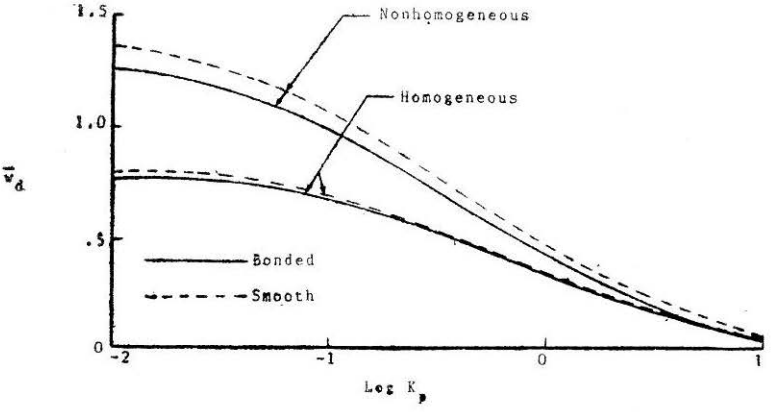

FIGURE 21 Effect of Nonhomogeneity and K_p on the Variation of Maximum Differential Displacement of Partially Embedded Foundation, for $V_s=0.3$.

except in the case of the central moment where the effect of soil nonhomogeneity is not very significant (Fig. 22).

The radial moment variation along the tank wall is shown in Fig. 23 and 24. At the plate-wall junction, for $K_p = 0.01$ and for a rough plate-soil contact, the radial moment for the nonhomogeneous soil assumption is about 23.4% higher, while for a smooth plate-soil contact, it is about 31.7% higher than the corresponding value for the homogeneous soil assumption.

Effect of Soil Nonlinearity

The hyperbolic relation used in this study represents the nonlinear behaviour of soil in terms of two material constants *a* and *b*. The following

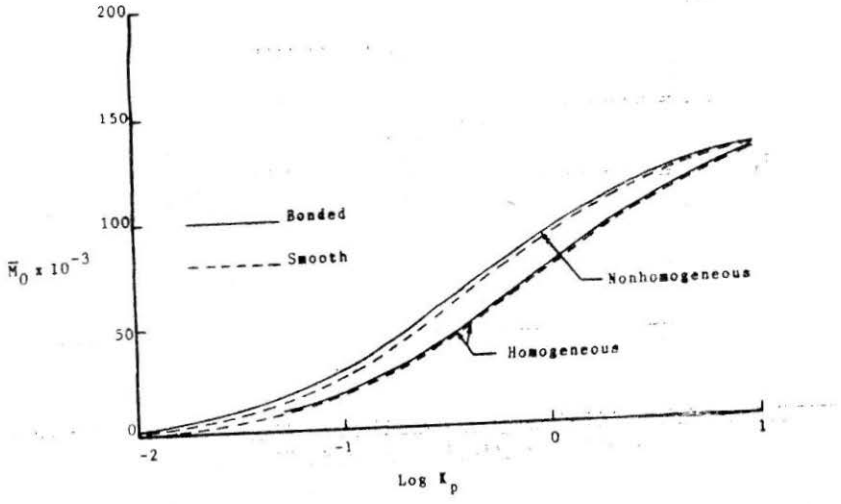

FIGURE 22 Effect of Nonhomogeneity and K_p on the Variation of Central Moment of a Partially Embedded Foundation, for $V_p=0.3$.

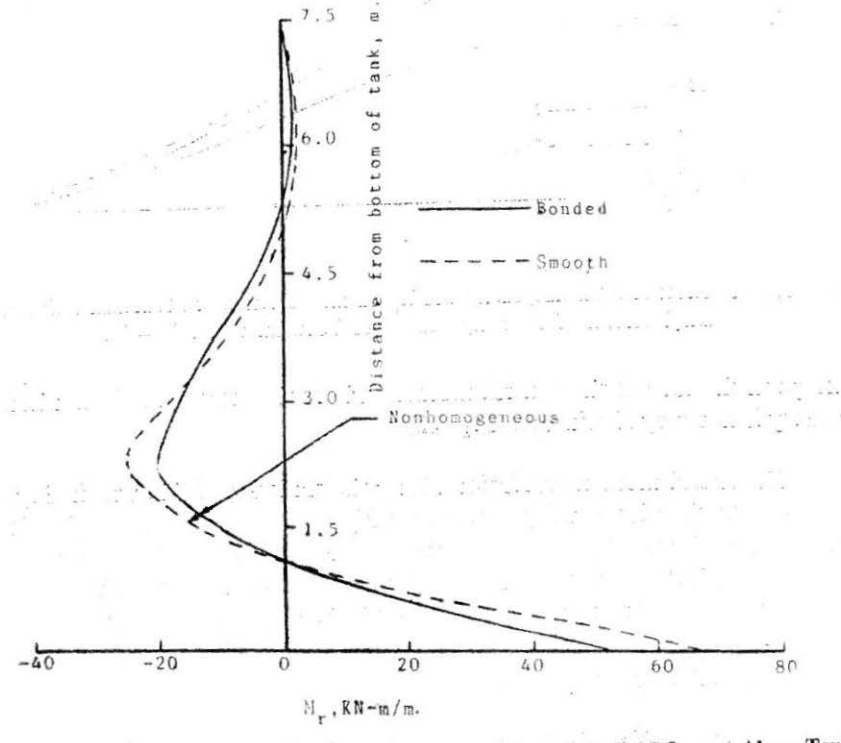

FIGURE 23 Effect of Interface Condition on the Variation of Radial Moment Along Tank Wall, for $K_p=1$ and Homogeneous Soil, for $V_s=0.3$.

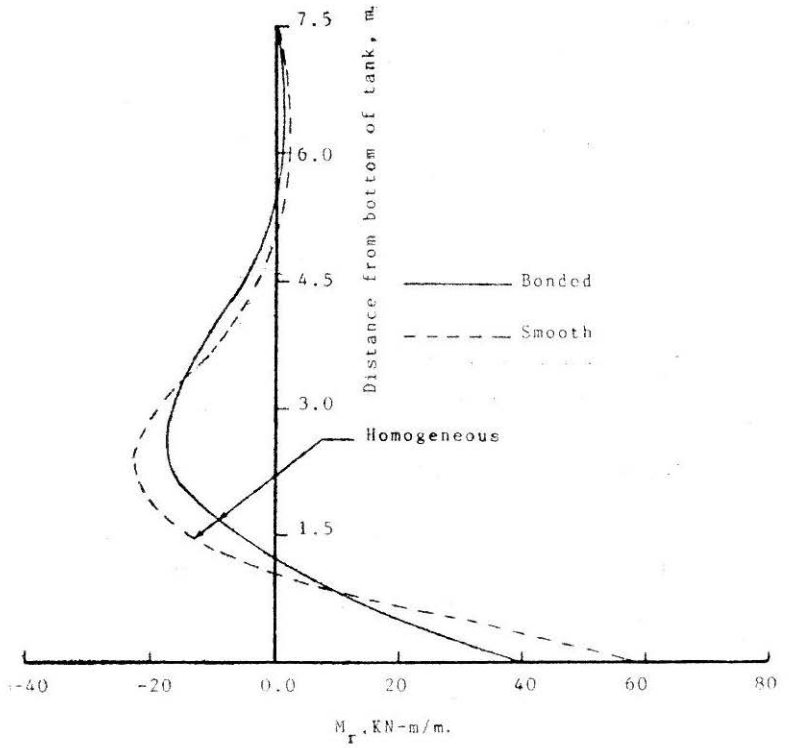

FIGURE 24 Effect of Interface Condition on the Variation of Radial Moment Along Tank Wall, for K_p=1.0 and Nonhomogeneous Soil, for V_s=0.3.

values (Desai and Siriwardane (1984), Kondner (1963)) were used in the parametric study: $a = 0.00021$ and $b = 0.01$.

Typical results obtained from this parametric study are presented in Figs. 25 through 29. Figure 25 shows the variation of central plate displacement with relative rigidity of the plate. $\bar{w}_o$ obtained for the nonlinear soil medium is higher than the corresponding value for the linear soil, the difference being less significant at higher K_p. $\bar{w}_o$ for bonded plate-soil contact is about 17% less for the linear soil assumption at $K_p = 0.01$, whereas it is only 7% less for $K_p = 10$. The effect of the interface is seen to be slightly more prominent for the nonlinear soil medium. Figure 26 shows the variation of maximum differential plate displacement with K_p. $\bar{w}_d$ shows a similar trend of variation. At high plate relative rigidity, the difference between the nonlinear and linear cases becomes insignificant. Figure 27 shows the variation of the central plate moment. At lower plate relative rigidities, the nonlinear soil assumption results in higher values of the central moment, but the trend is reversed when the plate becomes very rigid. Figures 28 and 29 show the effect of soil nonlinearity on the variation of radial moment along the tank wall.

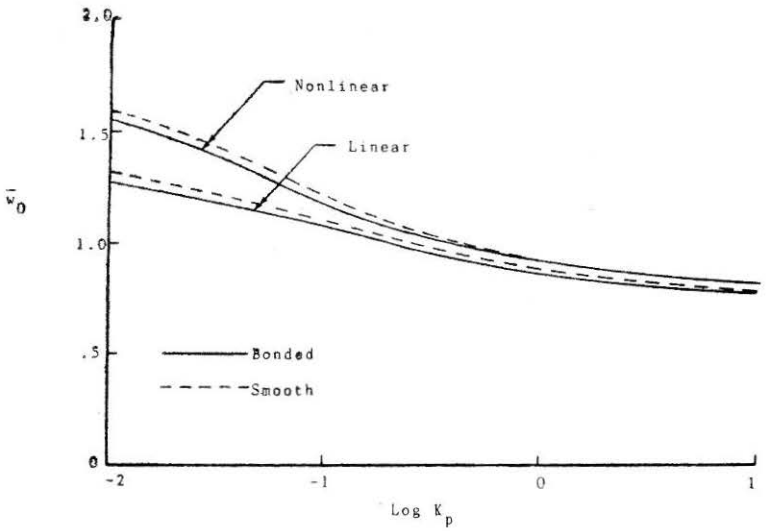

FIGURE 25 Effect of Soil Nonlinearity and Relative Rigidity K_p on the Variation of Central Displacement of a Partially Embedded Foundation.

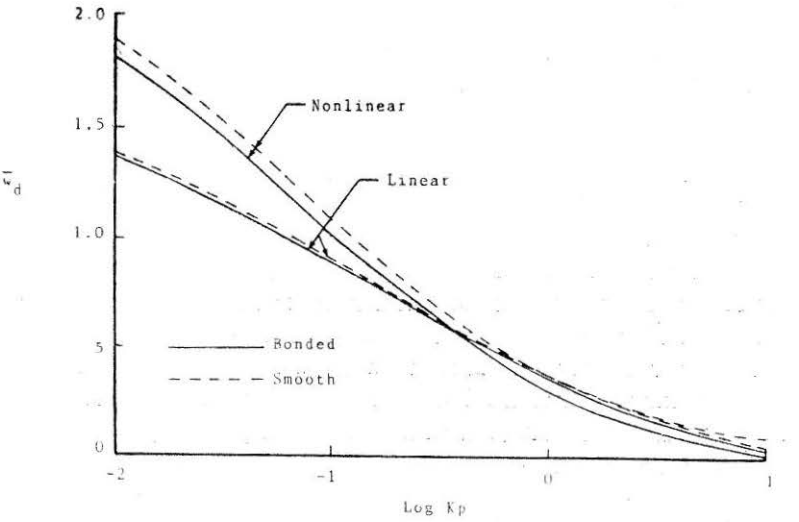

FIGURE 26 Effect of Nonlinearity and K_p on the Variation of Maximum Differential Plate Displacement of a Partially Embedded Foundation.

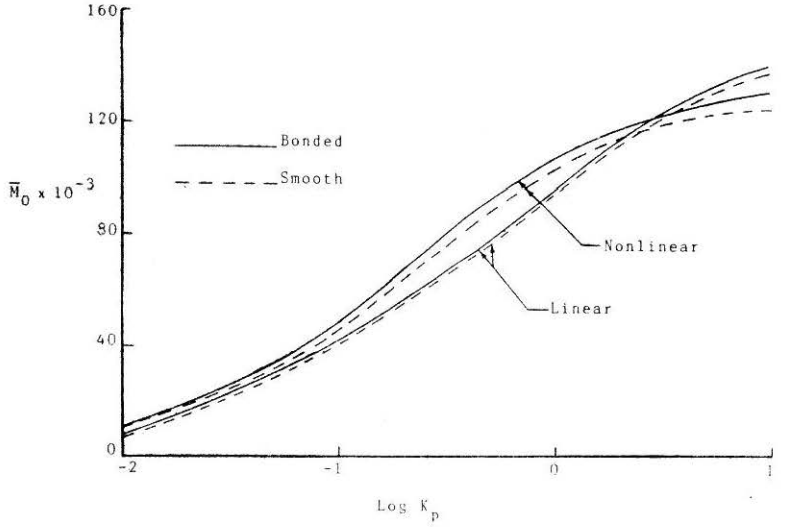

FIGURE 27 Effect of Nonlinearity and K_p on the Variation of Central Moment of a Partially Embedded Foundation.

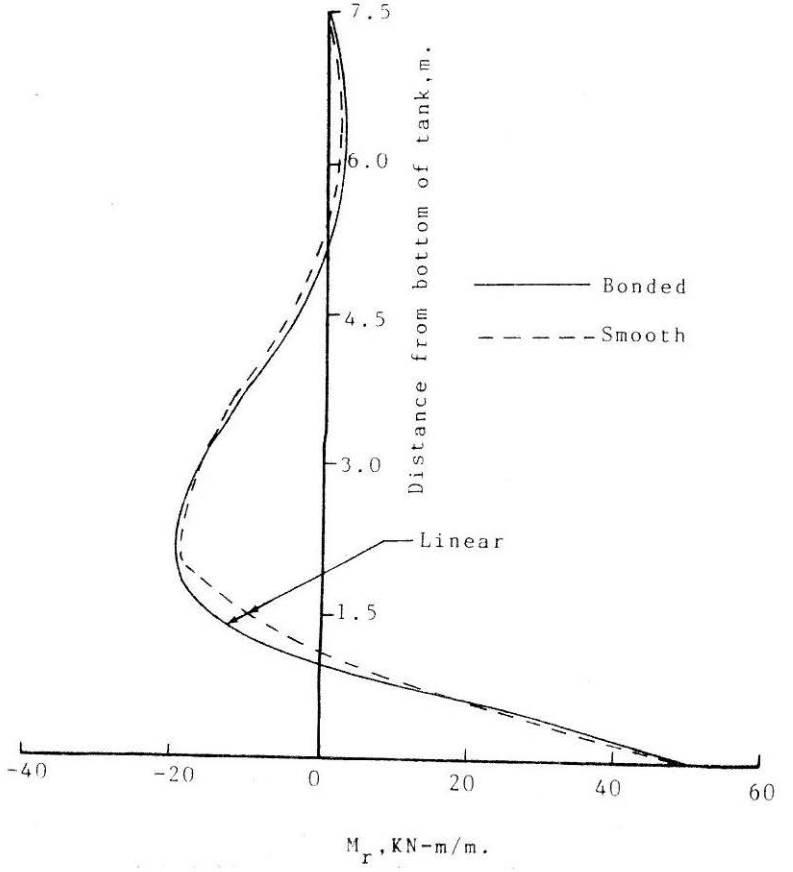

FIGURE 28 Effect of Interface Roughness on the Variation of Radial Moment Along Tank Wall, for K_p=1 and Linear soil.

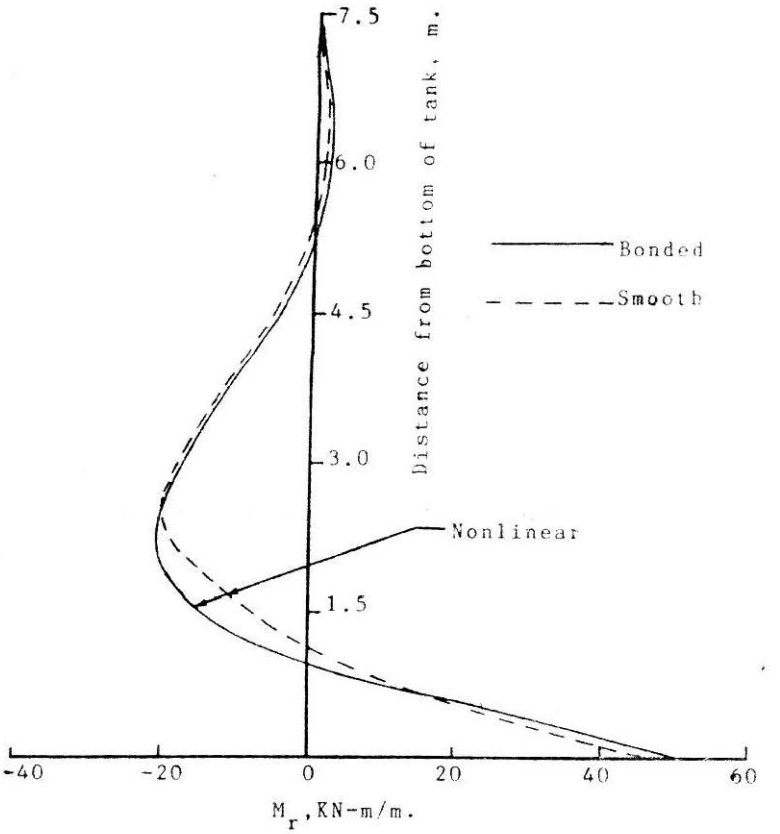

FIGURE 29 Effect of Interface Roughness on the Variation of Radial Moment along Tank Wall, for K_p=1 and Nonlinear Soil.

Conclusions

The objective of this paper was to examine the behaviour of cylindrical storage tanks resting on or partially embedded in an isotrophic soil medium, considering the possible interactions between the tank wall, circular foundation and soil medium. Emphasis was given to modelling the nonlinear behaviour of soils and interfaces. Based on the numerical results presented in the preceding section, the following conclusions can be made:

1. Central, as well as differential deflection of a cylindrical tank foundation decreases with the increase in its relative rigidity. However, flexural moments increase with the increasing relative plate rigidity.

2. Neglecting the presence of the tank wall results in a conservative estimate of deflections in the central region of the foundation.

3. In many situations, assuming soil to be homogeneous may result in gross error in estimation of foundation responses.

4. Response of cylindrical tank foundations can be significantly affected by soil nonlinearity. An analysis procedure based on linearly elastic soil properties underestimates the actual response.

5. Likewise, the response of circular foundations is influenced by the interface conditions. Smooth interface conditions result in increased foundation deflection.

6. The interface roughness has more pronounced effects on foundation reponse at lower Poisson's ratios of halfspace. These effects are significantly reduced as the halfspace tends to become incompressible ($v_s \rightarrow 0.5$).

7. Vertical (normal) stress distribution in soil beyond a certain depth becomes independent of any of the parameters studied herein.

8. In general, the interface condition appears to have more influence on the flexural behavior of foundations, when soil nonlinearity is considered in the analysis.

REFERENCES

BATHE, K.J. (1982), "*Finite Element Procedures in Engineering Analysis*," Prentice-Hall, Inc., Englewood Cliff, N.J.

BEER, G. (1985), "An Isoparametric Joint/Interface Element for Finite Element Analysis," (*Int. J. for Num. Met. in Engng.*, 21, 585-600.

BOOKER, Jr. R. and SMALL, J.C. (1983), "The Analysis of Liquid Storage Tanks on Deep Elastic Foundations," *Int. J. for Num. and Anal. Met. in Geomech.*, 7, 187-207.

BROWN, P.T. (1969), "Numerical Analysis of Uniformly Loaded Circular Rafts on Deep Elastic Foundations," *Geotechnique*, 19, 3, 399-404.

DESAI, C.S. and SIRIWARDANE, H.J. (1984), "*Constitutive Laws for Engineering Materials with Emphasis on Geologic Materials*," *Prentice-Hall, Englewood* Cliff, N.J.

FARUQUE, M.O. (1980), "The Role of Interface Element in Finite Element Analysis of Geotechnical Engineering Problems," *M.S. Thesis*, Carleton University, Canada.

FINELLI, G.B. and PICARELLI, L. (1984), Letter to the Editor, Int. J for. Num. and Anal. Met. in Geomech., 8, 3, 305-306.

GHABOUSSI, J., WILSON, E.L. and ISENBERG, J. (1973), "Finite Elements for Rock Joints and Interfaces," *ASCE J. of Soil Mech. and Fdn. Div.*, 99. SM 10, 833-848.

HOOPER, J.A. (1974), "Analysis of a Circular Raft in Adhesive Contact with a Thick Elastic Layer," *Geotechnique*, 24, 4, 561-580.

HOOPER, J.A. (1975), "Elastic Settlements of a Circular Raft in Adhesive Contact with a Transversely Isotropic Medium," *Geotechnique*, 25, 4, 691-711.

ISSA, A. (1985), "Analysis of Cylindrical Storage Tanks and Circular Plate Foundations Resting on Isotropic Elastic Halfspace Using an Energy Method", *M. Eng. Thesis*, Univ. of Oklahoma, Norman, OK.

ISSA, A. and ZAMAN, M.M. (1985), "A Cylindrical Tank-Foundation-Halfspace Interaction Using an Energy Approach," *Computer Met. in Applied Mech. and Engng.*, 56, 47-60.

KONDNER, R.L. (1963a) "Hyperbolic Stress-Strain Relation for Cohesive Soils," *J. of Soil Mech. and Fdn. Div., ASCE*, 89, SM 1, 115-143.

KONDNER, R.L. and ZELASKO, J.S. (1963b), "A Hyperbolic Stress-Strain Formulation for Sands," *Proc. 2nd Pan American Conf. on Soil Mech. and Fdn. Engng.*, Brazil, 1, 289-324.

MAHMOOD, I.U. (1984), "Finite Element Analysis of Cylindrical Tank Foundations Resting on Isotropic Soil Medium Including Soil-Structure Interaction," *M. Eng. Thesis*, Univer. of Oklahoma, Norman, OK.

SELVADURAI, A.P.S. (1979a), "The Interaction Between a Uniformly Loaded Circular Plate and an Isotropic Elastic Halfspace: A Variational Approach," *J. of Struct. Mech.*, 7, 231-246.

SELVADURAI, A.P.S. (1979b), "*Elastic Analysis of Soil-Foundation Interaction*," Developments in Geotech, Engng., 17, Elsevier Scientific Publishing, Amsterdam.

SELVADURAI, A.P.S. and FARUQUE, M.O. (1981), "The Influence of Interface Friction on the Performance of Cable Jacking Tests of Rock Masses," *Proc. Impl. of Comp. Procedures and Stress-Strain Laws in Geotech. Engng.*, Chicago, I, 169-183.

TIMOSHENKO, S.P. and WOINOWSKY-KRIEGER (1959), "*Theory of Plates and Shells*," McGraw-Hill, New York.

ZAMAN, M.M., KUKRETI, A.R. and ISSA, A. (1988), "Analysis of Circular Plate-Elastic Halfspace Interaction Using an Enegy Approach," Applied Mathematical Modeling, 12, 285-292.

ZAMAN, M.M. and ISSA,A. and MAHMOOD, I.U. (1985), "Analysis of Cylindrical Structure Foundation Interaction Using Variational Approach," *Proc. 2nd Int. Conf. on Variational Met. in Engng.*, held in Southampton, England, 17-19, 12-1 - 12-12.

ZEMOCHKIN, B.N. (1939), "*Analysis of Circular Plates on Elastic Foundation*," Mosk, Izd. Voenno, Inzh. Akad., Moscow.

ZIENKIEWICZ, O.C., (1971), "*The Finite Element Method*," McGraw-Hill, New York.